Indian Journal of Orthopaedics (2025) 59:2088–2098
https://doi.org/10.1007/s43465-025-01568-2

ORIGINAL ARTICLE

Circulating miR-19b in Serum Exosomes: A Novel Biomarker for Estrogen-Associated Osteoporosis

Chitravel Renuka[1] · Kirubamani Palanichamy[2] · Sathish Muthu[3,4] · Chithravel Vadivalagan[5]

Received: 15 March 2025 / Accepted: 16 July 2025 / Published online: 25 September 2025
© Indian Orthopaedics Association 2025

Abstract

Introduction Osteoporosis, a significant health concern among postmenopausal women, is influenced by estrogen deficiency, which affects bone metabolism. Current diagnostic methods, such as dual-energy X-ray absorptiometry (DXA), have limitations in sensitivity, necessitating the identification of novel biomarkers for early diagnosis. This study investigates the role of circulating exosomal miR-19b as a potential biomarker for estrogen-associated osteoporosis.

Methods We analyzed the expression of miR-19b in MC3T3-E1 preosteoblast cells treated with 10 pM estradiol and assessed its antagonistic effects using 10 nM anastrozole. Serum exosomes were isolated from premenopausal (PR-M) and postmenopausal (PT-M) women using microfluidics-based extracellular vesicle (EV) isolation. Exosomal miR-19b expression was quantified using qRT-PCR, and its correlation with age, estrogen levels, and osteoporosis risk was evaluated. Characterization of exosomes was performed using transmission electron microscopy (TEM) and tunable resistive pulse sensing (TRPS), while protein markers CD9, CD63, and β-actin were confirmed through Western blot analysis.

Results Our findings demonstrate that estrogen downregulates exosomal miR-19b expression, with a significant difference observed between the PR-M and PT-M groups. Receiver operating characteristic (ROC) analysis revealed that miR-19b effectively differentiates between these groups, with an area under the curve (AUC) of 0.9911. Pearson correlation analysis further confirmed the strong association between miR-19b expression, estrogen levels, and age. Additionally, miR-19b inhibition was found to regulate IGF-1 expression, influencing bone cell differentiation and osteoporosis progression.

Conclusion This study establishes exosomal miR-19b as a novel biomarker for estrogen-related osteoporosis, providing a foundation for early diagnosis and therapeutic targeting. Our findings highlight the potential of exosomal miRNAs in advancing precision medicine for osteoporosis management.

Keywords Osteoporosis · Estrogen · Exosomes · miR-19b · Biomarker · Bone metabolism · Postmenopausal women

Introduction

Studies on Indian women of various ages have found that the prevalence of osteoporosis ranges from 8 to 62% [1, 2]. The primary method used for diagnosing osteoporosis in India, as recommended by the Indian Society for Bone and Mineral Research (ISBMR), is dual-energy X-ray absorptiometry (DXA), which measures bone mineral density (BMD) [3]. Single- or dual-energy absorptiometry may be used to evaluate bone mineral density, which is a useful diagnostic tool for osteoporosis. These measures have a reduced sensitivity even if they have a high specificity. As a result, the method is especially useful for determining who is more susceptible to osteoporosis [4, 5]. Several diagnostic tools and techniques are used to diagnose osteoporosis, but one important molecular

✉ Chitravel Renuka
renukaphd@gmail.com

1 PG and Research Department of Zoology, Nehru Memorial College, Puthanampatti, 621007 Trichy District, Tamil Nadu, India

2 International PhD Program in Biomedical Engineering, College of Biomedical Engineering, Taipei Medical University, New Taipei City 235603, Taiwan

3 Orthopaedic Research Group, Coimbatore, Tamil Nadu, India

4 Central Research Laboratory, Meenakshi Medical College Hospital and Research Institute, Meenakshi Academy of Higher Education and Research, Chennai, India

5 Department of Surgery, University of Michigan Medical Centre, Ann Arbor, MI, USA

strategy is the identification of certain biomarkers including serum osteocalcin, alkaline phosphatase, osteoprotegerin, RANKL, COL1A1, and COL1A2. In general, these genetic and biochemical indicators are more accurate at identifying osteoporosis [6]. To prevent and monitor, however, we require early tools for diagnosis [6]. The possible involvement of microRNAs (miRNAs) in bone homeostasis control, bone remodeling, bone resorption, and bone cell differentiation has been shown. The pathophysiology of bone illnesses like osteoporosis may thus be impacted by altered expression of several miRNAs [7]. While traditional tools like DXA provide structural insight into bone mass, they often lack the sensitivity for early-stage detection [6]. This has sparked an interest in molecular diagnostics, including biochemical and genetic markers. Among these, microRNAs (miRNAs)—small non-coding RNAs involved in post-transcriptional regulation—have emerged as key players in skeletal homeostasis [8]. miRNAs such as miR-19b are implicated in the regulation of osteoblast and osteoclast function, thus influencing bone remodeling dynamics [9].

Exosomes are cell-derived vesicles that contain a wide range of active biomolecules, which include nucleic acids, proteins, lipids, mRNAs, cellular receptors, and immunological regulatory components. Their diameters normally vary from 30 to 150 nm. Exosome surfaces may be modified in a variety of ways, including the addition of peptides, fluorescent dyes, and antibodies, to facilitate the transport of both big and tiny biological products [10]. By sending and/or receiving signals that can change cellular metabolism and regulate receptor signalling complexes, exosomes enable cellular communication [11]. Interestingly, these miRNAs are also enriched in serum-derived exosomes, which serve as stable carriers of intercellular signals, including hormonal cues like estrogen [8]. This molecular cross-talk offers an untapped opportunity for early osteoporosis detection.

In adult bone, estrogen is crucial for bone development and maturation as well as for controlling bone turnover. In both males and females, estrogen is required for the appropriate closing of the epiphyseal growth plates during bone growth. Increased osteoclast production and greater bone resorption are also caused by estrogen deprivation in the juvenile skeleton [12, 13]. Among estrogen-responsive miRNAs, miR-19b has gained attention for its role in modulating transcription factors such as Sp-1 (specificity protein 1) and pathways involved in bone metabolism [14]. Sp-1 is a transcription factor that mediates the expression of several bone-related genes and estrogen receptor targets. miR-19b is known to modulate Sp-1 expression, and this regulatory relationship is particularly relevant in the context of estrogen deficiency-induced bone loss. Its expression has been shown to be altered in osteoporotic conditions and is detectable in serum exosomes, making it a potential candidate for non-invasive diagnostics [14]. In this study, we investigate the exosome-mediated signal transduction mechanisms of estradiol in bone remodeling. As illustrated in Fig. 1, we show how estradiol inhibits miR-19b targeting and affects Sp-1 transduction signals via estrogen receptor elements in the progesterone receptor gene. MicroRNAs play a crucial role in post-transcriptional regulation through various molecular pathways. In our study, we assessed the expression of the target miR-19b in MT3T3-E1 cells, measuring its levels in response to 10 pM estradiol and evaluating its potential antagonistic effects using anastrozole. We analyzed serum exosomal miR-19b expression in both premenopausal and postmenopausal women and assessed the diagnostic value of estrogen-associated exosomal miR-19b using an independent cohort. Exosomes were isolated from the serum of these women, who had an average age of 45.85 (ranging from

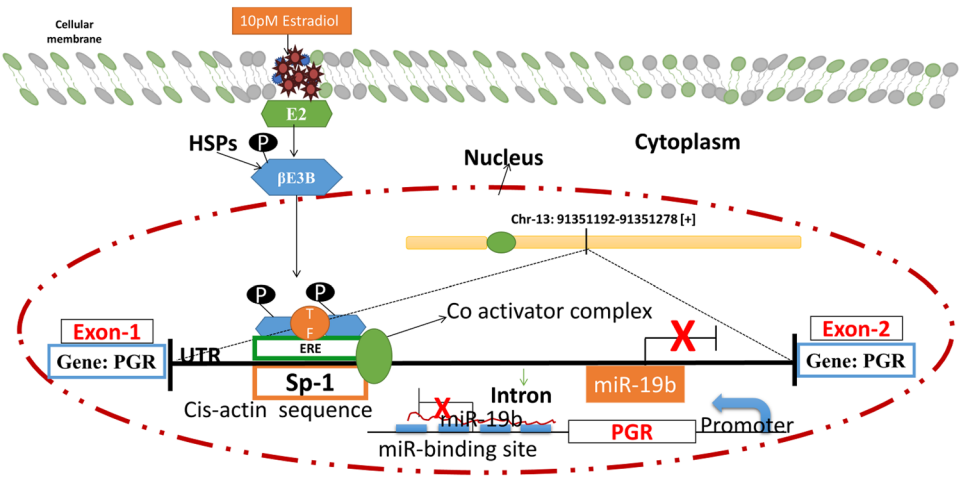


Fig. 1 Molecular mechanism of estradiol-mediated exosomal miR-19b target inhibition in MT3T3-E1 cells and human serum

32 to 54) and 65 (ranging from 55 to 77) years, using the microfluidics-based EV isolation method. The study aimed to identify serum-derived exosomal miR-19b as a biomarker for osteoporosis and evaluate its diagnostic performance concerning estrogen levels.

Material and Methods

Major Reagents and Antibodies

Dulbecco's modified Eagle's medium (DMEM), fetal bovine serum (FBS), and antibiotic penicillin, streptomycin, and L-glutamine (PSG) were supplied by GIBCO (BRL/Invitrogen, Carlsbad, USA). Estradiol/β-estradiol and anastrozole were from Millipore Sigma, USA.

Cell Culture and Drug Treatment

Preosteoblast MC3T3-E1 cells were cultured in DMEM containing 10% of heat-inactivated FBS, 1% of PSG (penicillin (100 IU/mL), streptomycin (100 mg/mL), and L-glutamine (2 mM)). Cells were suspended in a 6-cm Petri dish under a 5% CO_2 humidified atmosphere at 37 °C. 1×10^5 of MCT3T-E1 cells were initially seeded into a 6-cm Petri dish with DMEM and after 24 h the differential reagents (as described above) were treated up to 24 h and the culture medium was harvested at the 24th h for further exosome isolation analysis. 10 pM estradiol concentration was fixed after exposure to find out the time- and concentration-dependent effects. Similarly, 10 nM anastrozole was fixed to evaluate its potential antagonistic effects.

Serum Samples

Serum samples were obtained from Government Medical College and Hospital, Dindigul, TN, India, from individuals who were linked to premenopausal (PR-M) ($n = 14$) and (postmenopausal) PT-M ($n = 16$). The Institutional Medical Review Board, no. 2023/EC/R-0115, dated August 07, 2023, certified the ethical clearance. Every clinical characteristic of every donor is included in Table 1. Furthermore, all the other clinical values such as parity, BMI, and estrogen values are summary statistics that were used to define the characteristics of the donors.

Isolation and Characterization of Exosome

Exosomes were isolated from cultured medium with previously described methods by Thery et al., 2006. A slightly modified protocol was followed, the cell cultured medium was replaced with a fresh complete medium with 10% FBS in the control group, the differentiated group was additionally treated with testosterone with different concentrations, and the medium was harvested at the designated time. The centrifugation was initially performed at 350*g* for 10 min at 4 °C, followed by 2000*g* for 30 min at 4 °C. Further, the supernatant was centrifuged at 16,500*g* for 20 min at 4 °C. The collected supernatant was filtered with a 0.22 µm pore filter and centrifuged at 120,000*g* for 70 min at 4 °C. After centrifugation, small yellow pellets that appeared were dissolved in PBS. For the purification of the products, the final centrifugation step was repeated. Finally, the supernatant was discarded and air-dried at room temperature for 20 min. The pellet was resuspended with PBS (pH 7.4) and stored at −80 °C for downstream application.

Exosome Characterization

The extracted exosomes were characterized by two different approaches, which include particle size analysis and morphometric analysis.

Tunable Resistive Pulse Sensing (TRPS)

The particle size was analyzed using qNano (Izon Science Ltd, New Zealand), using the basic principles with tunable resistive pulse sensing [15]. The equipment calibration followed the manufacturer's protocol. 2× PBS was used as

Table 1 Clinical characteristics of individual women donors with basic estrogen levels

Variable	Premenopausal (PR-M)	Postmenopausal (PT-M)	*P*-value
N	14	16	
Age	45.85 (32, 54)	65 (55, 77)	< 0.0001***
Parity	P1 (6) P2 (8)	P1 (4) P2 (11) P3 (1)	0.543
Tobacco usage	2.00	3.00	0.432
Alcohol	1	1	0.651
BMI	23.4 ± 1.2	24.1 ± 2.1	0.321
Estrogen level (pg/mL)	44.57 (20, 120)	12.31 (7, 20)	< 0.0001***
Total estimates	−3.239 ± 3.07	0.5990 ± 1.6	0.3226
Estro. + estimates	0.1712 ± 0.15	−1.590 ± 0.44	0.0070**

an electrolyte with five dilutions. Polyurethane nano-pore ranked for particles mean 100 nm (NP150 Izon) was used and axially stretched to 48 × 54 mm. 100 µL of sample was diluted to an appropriate particle content in PBS. The measurement durations exceeded 10 minutes, and the instrument was calibrated using 120 nm standards.

For particle size, calibration was done using the formula:

$$\text{Particle volume:} \frac{dI(\text{sample})}{dI(\text{calibration, mean})} \times \text{calibration volume (mean)},$$

$$\text{Particle concentration: calibration concentration} \times \frac{\text{sample gradient}}{\text{calibration gradient}}.$$

Transmission Electron Microscopy (TEM)

Morphometric analysis was done using a transmission electron microscope (TEM) (Hitachi HT-7700-Core Facility Centre, TMU). In general, electron absorption is a basic principle to predict the structure using TEM. However, as exosomes have less electron-bound membrane, it was measured using an additional process called negative staining [16].

Western Blot Analysis

TEM and TRPS were two of the methods used to identify and characterize exosomes from cells and serum. To confirm their identification, a Western blot analysis was performed utilizing well-known extracellular vehicle (EV) surface markers, including CD9, CD63, and β-actin. Thermo Fisher supplied the β-actin (MA1-140), CD63 (10628D), and CD9 (10626D) antibodies utilized in this investigation. BSA was used as the reference standard in the Bio-Rad Protein Assay reagent as part of the standard methodology for protein measurement. SDS-PAGE (8–15% gel) was used to separate equivalent quantities of denatured protein samples (50–100 µg) for the Western blot analysis. The samples were then transferred overnight onto a PVDF membrane. The membrane was incubated for 30 min at room temperature with 5% nonfat dry milk powder in Tris-buffered saline with 0.1% Tween 20 (TBST) to prevent non-specific binding. Following blocking, primary antibodies were added to the membrane and incubated for the whole night at 4 °C. The membrane was incubated for 2 h with HRP-conjugated secondary antibodies (either goat anti-mouse or anti-rabbit) after the primary antibody was incubated. A stripping buffer was used to get rid of the bound primary antibodies so they could be probed again. The composition of the stripping buffer was pH 2.2, 0.1% SDS, 1.5% glycine, and 20% Tween 20. After gently rocking the membrane for 15 min at room temperature, the process was carried out three times, each time adding a new buffer. Following stripping, TBST was used to rinse the membrane three times for 10 min each. To evaluate the expression of certain proteins, the membrane was then re-blocked with 5% nonfat dry milk at room temperature for 30 min and incubated with primary antibodies.

Measurement of Micro-RNA (miR-19b) Expression

Total RNA Isolation

Following treatment, total RNA was extracted from MC3T3-E1 cells and exosomes using a slightly modified protocol. For the cells, 1 mL of TRIzol™ reagent was added to each treated 6-cm dish. For the culture medium, RNA was isolated by adding 100 µL of TRIzol™ reagent per 1 mL of medium. Samples were thawed and set for 10 min at RT before extraction. Initially, 0.2 mL of chloroform was thoroughly mixed by vortex and incubated for 3 min at RT and then the sample was centrifuged for 15 min at 12,000×*g* at 4 °C. The aqueous phase was transferred into a new tube and a further 0.5 mL of isopropanol was poured and mixed gently then incubated for 10 min at 4 °C and centrifuged for 10 min at 12,000×*g* at 4 °C. The total RNA precipitated forms a white gel-like pellet at the bottom of the tubes. The pellet was collected by discarding the supernatant, resuspended with 1 mL 75% ethanol, mixed by vortexing, and then centrifuged for 5 min at 7500×*g* at 4 °C. Finally, the supernatant was discarded and the RNA pellet was air-dried for 10 min and dissolved with DEPC water. The concentration of RNA was measured using a NanoDrop spectrometer at absorption under 260/280 and stored at −80 °C for further use.

Reverse Transcriptase PCR

Total RNA was used for cDNA synthesis with TaqMan primers specific for miR-93, using U6 as the internal control. The reaction mixture was prepared according to the manufacturer's instructions (Promega). For each reaction, the following components were used: 1.7 µL of DEPC-treated ddH2O, 2 µL of 5× reaction buffer, 1.2 µL of $MgCl_2$, 0.5 µL of dNTP mix, 0.1 µL of RNase inhibitor, 0.5 µL of reverse transcriptase (RT), 2 µL of TaqMan RT primer, and 2 µL of total RNA. The mixture was gently mixed and incubated on ice for 5 min. Reverse transcription was performed under the following conditions: incubation at room temperature for 5 min, 42 °C for 60 min, 85 °C for 5 min, and finally held at room temperature for 5 min. The resulting cDNA products were stored at −20 °C until further use.

Quantitative PCR Assays

The expression of miR-19b in human osteoblast was determined using qRT-PCR. After drug treatment, total RNAs were extracted and cDNA prepared for analysis of miR-19b and U6 snRNA. Oligonucleotide primers synthesized by Thermo Fisher (MI0000074-has-miR-19b; NR_004394 -U6 snRNA) were used and the reaction mixture was prepared as follows for each reaction: 10 µL TaqMan Universal master mix II (2×), 5 µL ddH_2O (DEPC treated), 1 µL of each primer (20×), 4 µL of cDNAs of each product, and total volume about 20 µL. Quantitative PCR amplification for miR-19b, miR-93 and U6 was performed with a standard running model of a 7500 Real-time PCR system. The product Ct values were correlated with the formula as follows: $\Delta Ct = Ct_{gene\ (miR\text{-}19b)} - Ct_{control\ (U6)}$, $\Delta\Delta Ct = \Delta Ct_{control} - \Delta Ct_{treated}$ and fold difference (2^−ΔΔCt).

Statistical Analysis

All statistical analyses were conducted using GraphPad Prism version 10.0.0 for Windows (GraphPad Software, San Diego, CA, USA). Data were expressed as mean ± standard deviation (SD). The statistical significance of differences between multiple experimental groups (e.g., control vs. drug-treated cells or premenopausal vs. postmenopausal cohorts) was assessed using a two-way analysis of variance (ANOVA), followed by Tukey's post hoc test to account for multiple comparisons. For associations between exosomal miR-19b expression levels and serum estradiol concentrations, Pearson's correlation analysis was performed, with significance set at a p-value < 0.05. All tests were two-tailed, and a p-value < 0.05 was considered statistically significant. Graphs were generated using the same software environment.

Results

The primary emphasis of the research was on the role that estrogen performed in the expression of miR-19b in MC3T3-E1 cells and the possibility of serum-derived exosomes/extracellular vesicles as an early biomarker for estrogen-based osteoporosis. To confirm the significance of miR-19b in the Indian population, we concentrated on assessing its expression in preosteoblast cells as well as serum-derived exosomes. Specifically, we examined this in connection to the impact of estrogen on osteoblasts. Our results showed an association between age, estrogen levels, and miR-19b expression.

We included 30 individual donors for this study, who were divided into the PR-M ($n = 14$) and PT-M ($n = 16$) groups. We validated miR-19b expression in preosteoblast cells, namely MT3T3-E1 cells, before examining serum samples. Ultracentrifuge (UC) method was employed for obtaining exosomes in a precise and efficient manner. When it comes to clinical samples, the UC approach is among the finest. Exosome characterization using TEM and TRPS is shown in Fig. 2, with both techniques showing that the particle size is between 50 and 150 nm. To confirm the existence of exosomes in the samples, western blotting using CD9, CD36, and ALX as possible immunoblotting markers for EVs was carried out and the results are discussed below.

The triangular expression by age, estrogen level, and miR-19b was scrutinized in this work, and our findings showed that estrogen affects the expression of miR-19b by downregulating the expressions depending on age. This study showed that exosomes and/or extracellular vesicles produced from MC3T3-E1 cell culture expressed miR-19b in response to estrogen. In the MC3T3-E1 cell-derived exosomes shown in Fig. 4, there is a time-dependent influence of 10 pM estradiol on the exosomal miR-19b expressions (Fig. 3).

Once the expression status of miR-19b in the MC3T3-E1 cells subjected to 10 pM estradiol/β-estradiol was confirmed, the cells were treated with an estrogen receptor inhibitor (10 µM anastrozole). The fold difference of the ΔΔCt value for each treatment, such as 10 pM estradiol, 10 µM anastrozole, and a combination treatment (10 pM estradiol + 10 µM anastrozole), was used to quantify the expression (Fig. 4). The expression of miR-19b in the exosomes derived from MC3T3-E1 cells was considerably affected after a 24-h treatment with a combined impact of 10 pM estradiol and 10 nM anastrozole. The chemical interaction of estrogen-to-estrogen transmitters in the nucleus is a key component of the ER's action mechanism. ERs dimerize first, and then they attach to certain response elements known as estrogen receptor elements (EREs).

The distribution of miR-19b expression within each group is graphically represented by the violin plot, which makes it possible to compare the central tendency, density, and distribution of data between PR-M and PT-M (Fig. 5A). Plotting the true positive rate against the false positive rate across a range of thresholds, the ROC curve assesses how well miR-19b expression separates these two circumstances. Using the area under the ROC curve (AUC) as a quantitative indicator of the miR-19b expression's capacity to distinguish between PR-M and PT-M, this method aids in evaluating the overall effectiveness of the expression (Fig. 5B). A thorough comprehension of the differences in miR-19b expression between the two groups and its potential as a diagnostic or prognostic biomarker is made possible by combining these statistical and visual assessments.

The scatter plot shows the miR-19b expression data for each group (Fig. 6A). When it comes to identifying the PR-M and PT-M groups based on estrogen levels, miR-19b's diagnostic

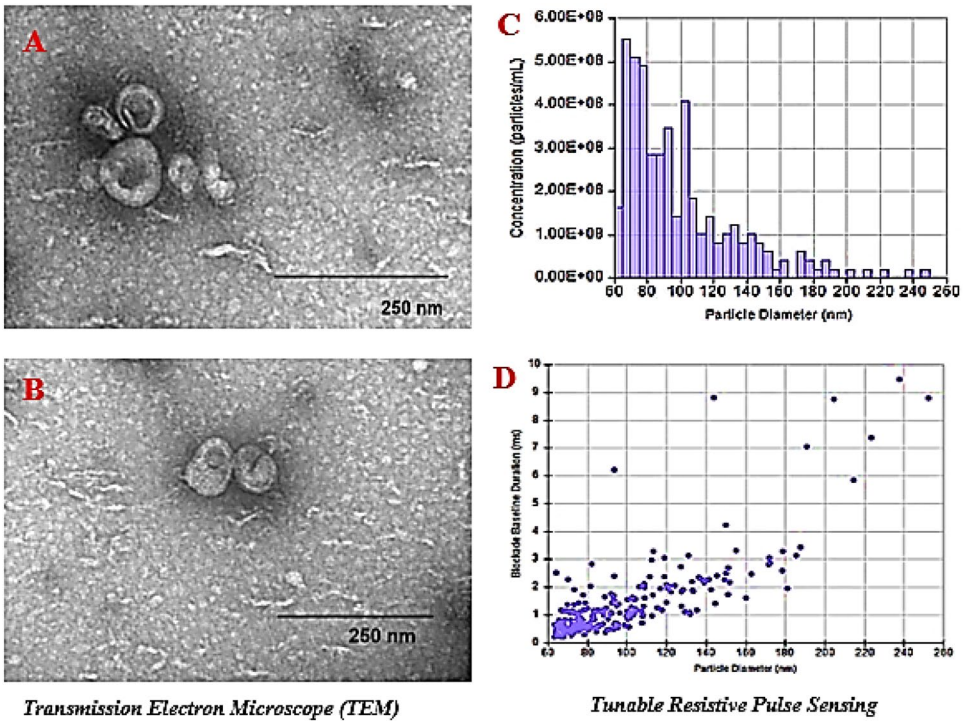


Fig. 2 Examination of exosomes isolated from human blood and derivatives of MC3T3-E1 cells. **A–B** Typical electron microscopy pictures following negative staining, displaying vesicles formations that ranged in size from 50 to 150 nm and were seen in every sample. Tunable resistive pulse sensing (**C–D**) demonstrating the vesicle concentration of particles per milliliter

performance is assessed using the ROC (receiver operating characteristic) curve (Fig. 6B). The true positive rate (sensitivity) versus the false positive rate (specificity) for different miR-19b expression thresholds were considered in the ROC curve. Better performance in separating the two groups according to the levels of miR-19b concerning estrogen levels in individual samples is shown by a bigger area under the ROC curve (AUC).

Additionally, we performed a correlation study utilizing multiple scatter plots and Pearson's correlation coefficient (r) to validate the association between miR-19b expression and estrogen levels. As seen in Fig. 7A and B, the analysis indicated significant variances with a p-value of less than 0.0001. We examined the relationship between the donors' ages and miR-19b expression for the final confirmation study, and the results showed that age had a major impact on the levels of miR-19b expression. Using a Pearson correlation value of −0.71, the scatter plots demonstrated a substantial upregulation of miR-19b expression in PR-M compared to age (Fig. 8a). When PR-M and PT-M were compared, the ROC curve showed substantial differences, with an AUC of 0.9911. Furthermore, with an AUC of 1.000, the correlation analysis between age, PR-M, and PT-M revealed a noteworthy improvement (Fig. 8b).

Discussions

Extracellular vesicles, also known as exosomes, are biosynthesized nanoparticles that contain a variety of genetic components, including snRNAs, fdDNAs, miRNAs, and fdRNAs. Based on differences in serum exosome miRNA expression between severe osteoporosis and normal bone mineral density in postmenopausal women, Shi et al. [17] provided evidence that profiling of miRNAs in exosomes reveals abnormal circulating miRNA levels in postmenopausal osteoporosis using second-generation sequencing. Osteoporosis development is suppressed by inhibition of miR-19b-3p functions in osteoporosis primarily by controlling IGF-1 gene expression [18]. In postmenopausal osteoporosis patients and BMSCs, the study evaluated the expression of miR-19b-3p, investigated its effects on cell proliferation and differentiation, and explored the possible connection between lncRNA H19 and miR-19b-3p [14]. By preventing BMSCs from differentiating into osteogenic tissues via the PTEN/Akt/mTOR autophagy pathway, our research indicates that miR-19b-3p overexpression leads to bone loss and recommends miR-19b-3p as a good target for treatment [19].

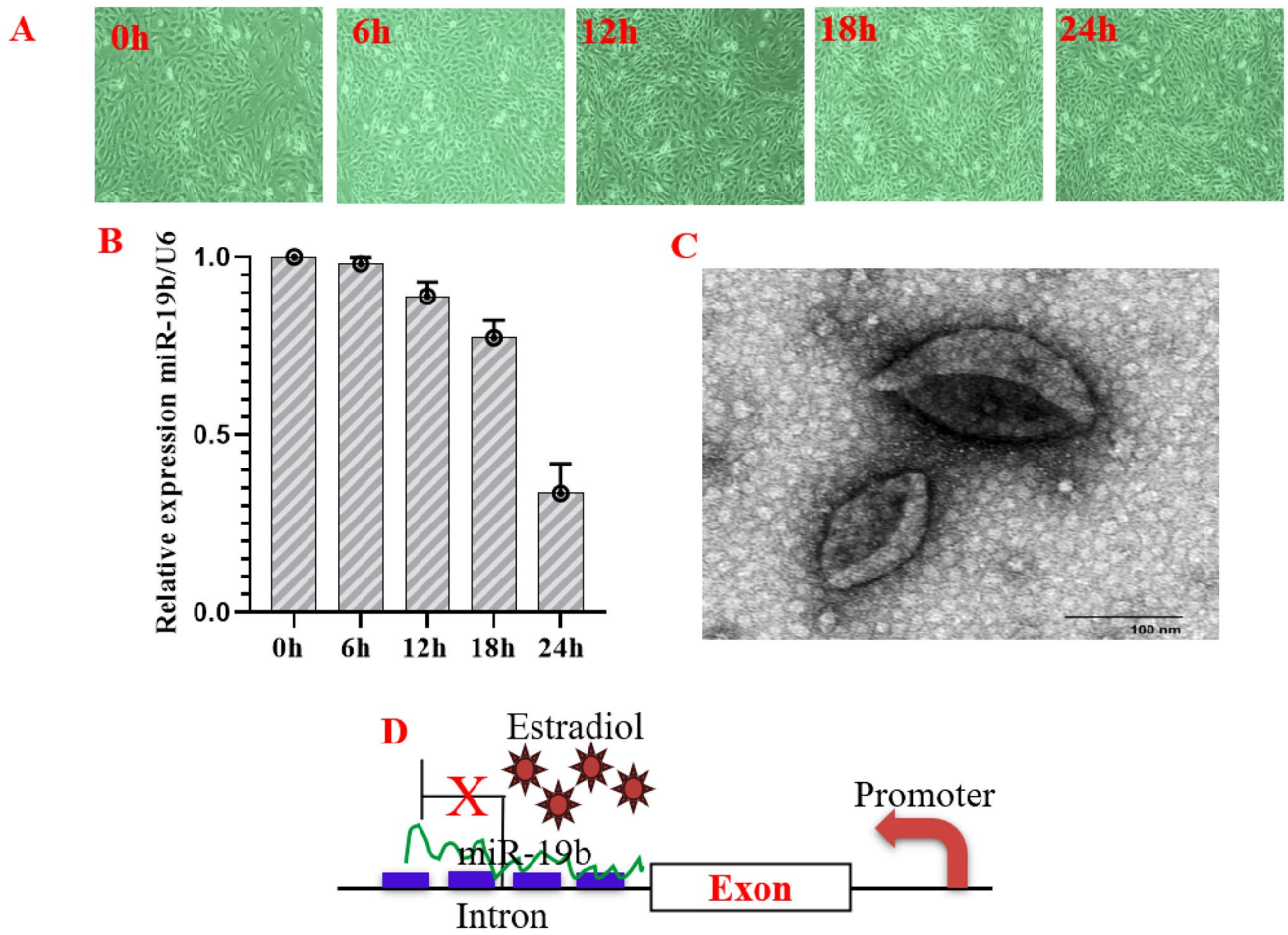


Fig. 3 Analysis of exosomes extracted from MC3T3-E1 cell derivatives. **A** Morphological examination of time interval differences. **B** The relative expression of the time-dependent impact caused by 10 pM estradiol on the expression of miR-19b in exosomes obtained from MC3T3-E1 cells. **C** Typical electron microscopy images after negative staining, showing the production of vesicles with sizes ranging from 50 to 150 nm. **D** Pictorial representation of estradiol transcription mechanism of action in miR-19b

Xiaoling et al. [14] observed that postmenopausal osteoporosis patients had significantly lower levels of lncRNA H19 expression. They also discovered that overexpression of H19 significantly suppressed BMSC proliferation by targeting miR-19b-3p. For the first time, the H19/miR-19b-3p axis was shown to play a significant role in osteoporosis in this work, providing a novel therapeutic target. According to Nilsson et al. [20], target gene promoters include EREs, and contact with ERs causes a conformational shift in the receptors' ligand-binding domain. Activator proteins may now be recruited thanks to this conformational shift [21]. We measured miR-19b utilizing changes in estrogen levels before and after anastrozole treatment, since the study highlighted the suppression of estrogens is related to this treatment.

The significant gene progesterone receptor's ERE transducing signal, which has an estrogen-inhibitory impact on miR-19b, has been further supported by this validation. To get a deeper comprehension of transcription factors, we verified our findings with the JASPAR database. It was observed that eight potential sites were predicted with a relative profile score threshold of 80%. We directly analyzed miR-19b expression in the Indian population based on all available data. To quantify miR-19b expressions, we used serum-derived EVs, which we then associated with age and estrogen levels. According to Sun et al. [22], circulating miR-19b is involved in promoting osteoblastogenesis and may be a valuable therapeutic target in bone loss disorders like osteoporosis. This is likely due to its ability to regulate the PTEN/pAKT/Runx2 pathway.

Certain miRNAs can be significant regulators of ER-dependent gene regulation because they selectively target estrogen receptors (ERs). As a case study, ERα expression is regulated by estrogen-induced miRNAs such as miR-18a, miR-19b, and miR-20b, which produce a loop of negative feedback [23]. It is commonly recognized that ERT is a successful therapy approach that slows the advancement

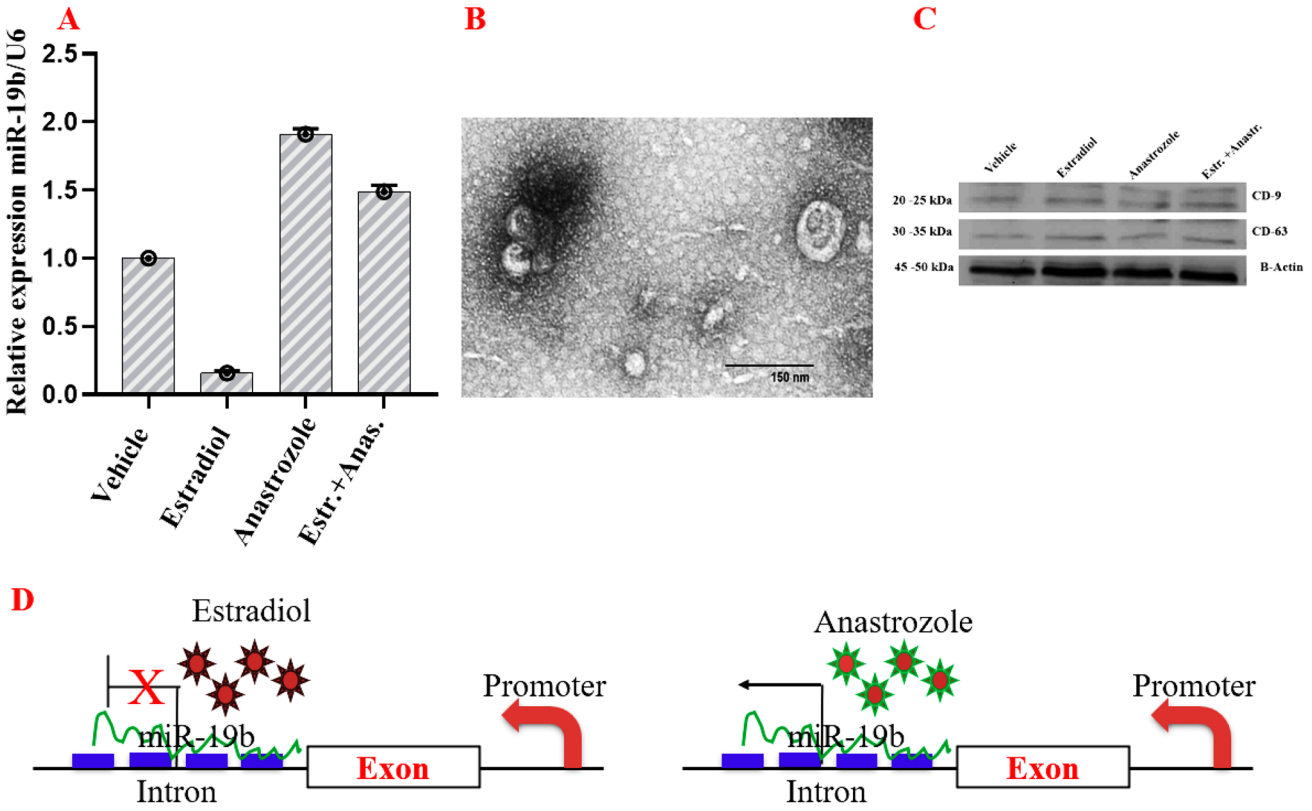


Fig. 4 Examination of exosomal miR-19b expressions taken from derivatives of MC3T3-E1 cells. **A** The influence of 10 pM estradiol, 10 nM estrogen receptor antagonist (anastrozole), and the combined effect of 10 pM estradiol and 10 nM estrogen receptor antagonist (anastrozole) on the expression of miR-19b in exosomes derived from MC3T3-E1 cells. **B** Representative electron microscopy pictures following negative staining, demonstrating the formation of vesicles ranging in size from 50 to 150 nm. **C** Using the traditional exosomal CD markers (CD9, CD63) and β-actin, a Western blot was carried out to evaluate the exosome presence in the MC3T3-E1 Cell derivatives. **D** Illustrative depictions of the miR-19b estradiol transcription mode of action

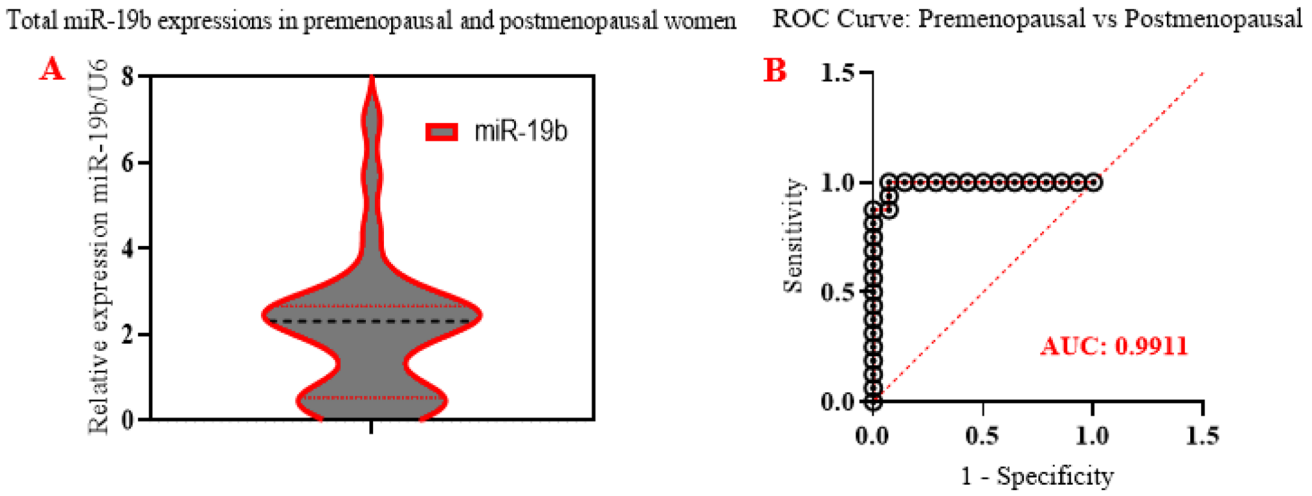


Fig. 5 **A** Overall miR-19b expressions in women identified as PR-M and PT-M. **B** The miR-19b receiver operating characteristics (ROC) curve combined with the PR-M and PT-M women in each donor. The AUC of 0.9911 indicates a significant difference with a 95% confidence interval (0.9678–1.000) between PR-M and PT-M, $P < 0.0001$

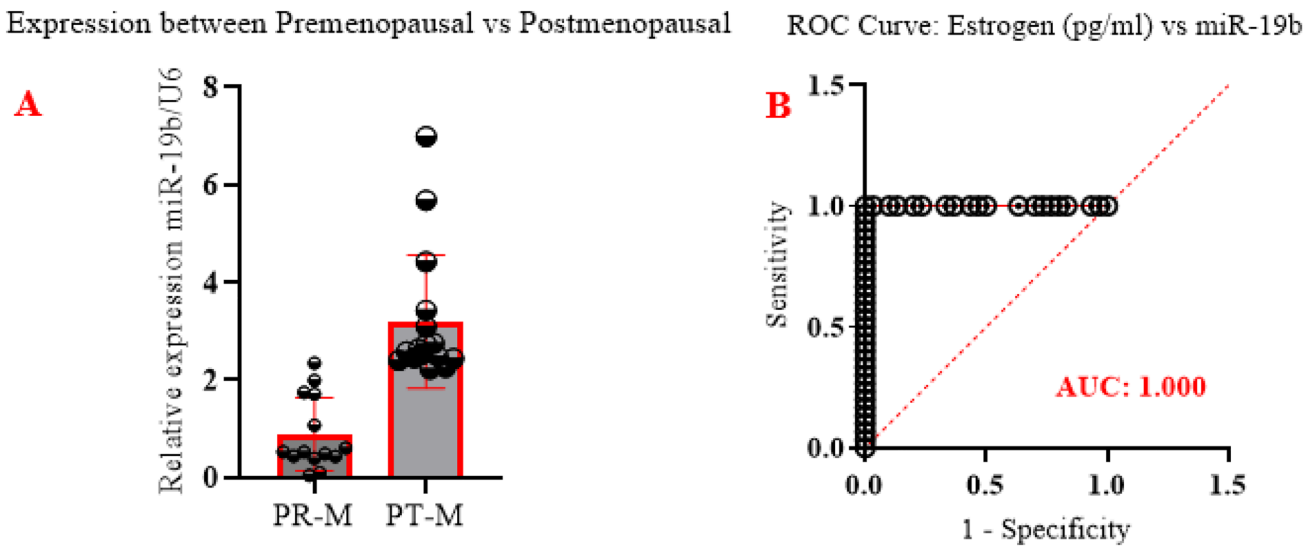


Fig. 6 **A** The individual miR-19b expressions between the PR-M and PT-M groups are represented by a scatter plot. **B** The receiver operating characteristics (ROC) curve for the miR-19b in combination with the estrogen vs. PR-M and PT-M women for every donor. With a 95% confidence interval (1.000 to 1.000) and an AUC of 1.000, there is a significant difference between PR-M and PT-M ($P < 0.0001$)

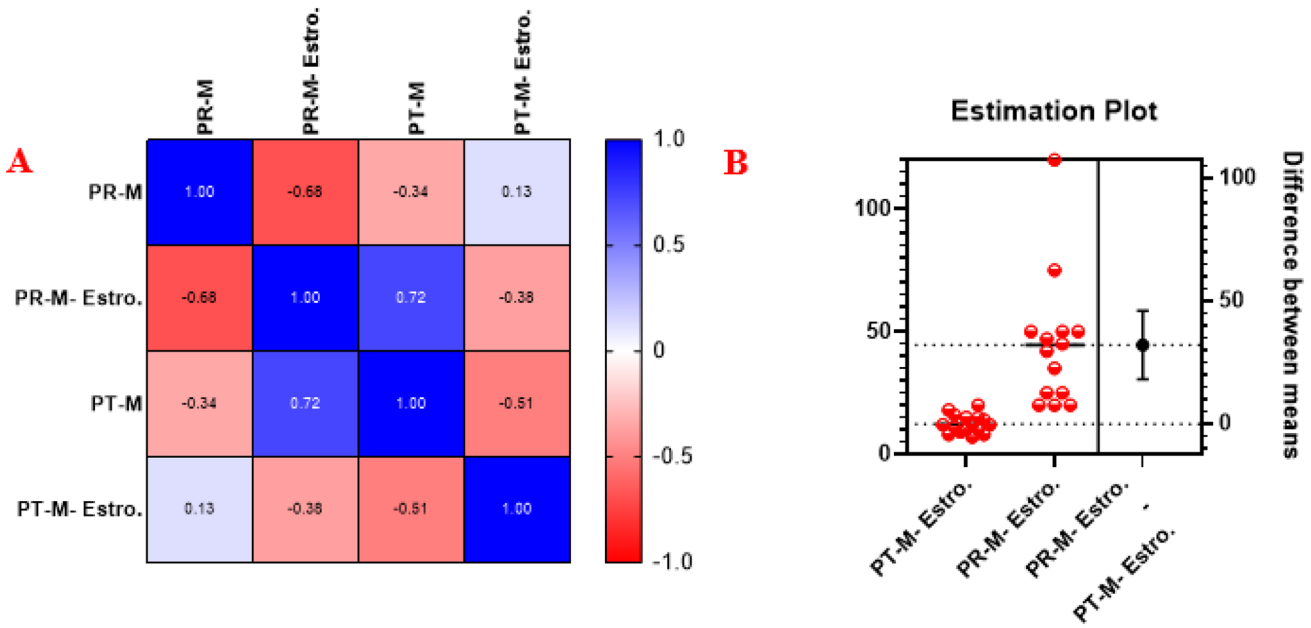


Fig. 7 The multiple matches scatter plot (**A**) illustrates the Pearson correlation coefficient (r) between miR-19b and estrogen in each of the four scenarios. **B** The individual miR-19b expressions between the estrogen vs. PR-M and PT-M groups are represented by a scatter plot. PR-M-PT-M means ± SEM (32.26 ± 6.775) two-tailed estimate difference between means with a 95% confidence interval (18.38-46.14), $P < 0.0001$

of osteopenia and avoids the development of osteoporosis and that estrogen protects against decreased bone density in both men and women [24]. Xiaoling et al. [14] reported that BMP-2-induced BMSCs and postmenopausal osteoporosis patients had significantly higher expression levels of miR-19b-3p.

While miR-19b-3p suppression reduced BMSC proliferation, overexpression of the protein significantly boosted it. Moreover, transfection with miR-19b-3p mimics markedly increased ALP activity and protein levels of RUNX2 and COL1A1, whereas transfection with miR-19b-3p inhibitors resulted in decreased levels of these markers. Additionally,

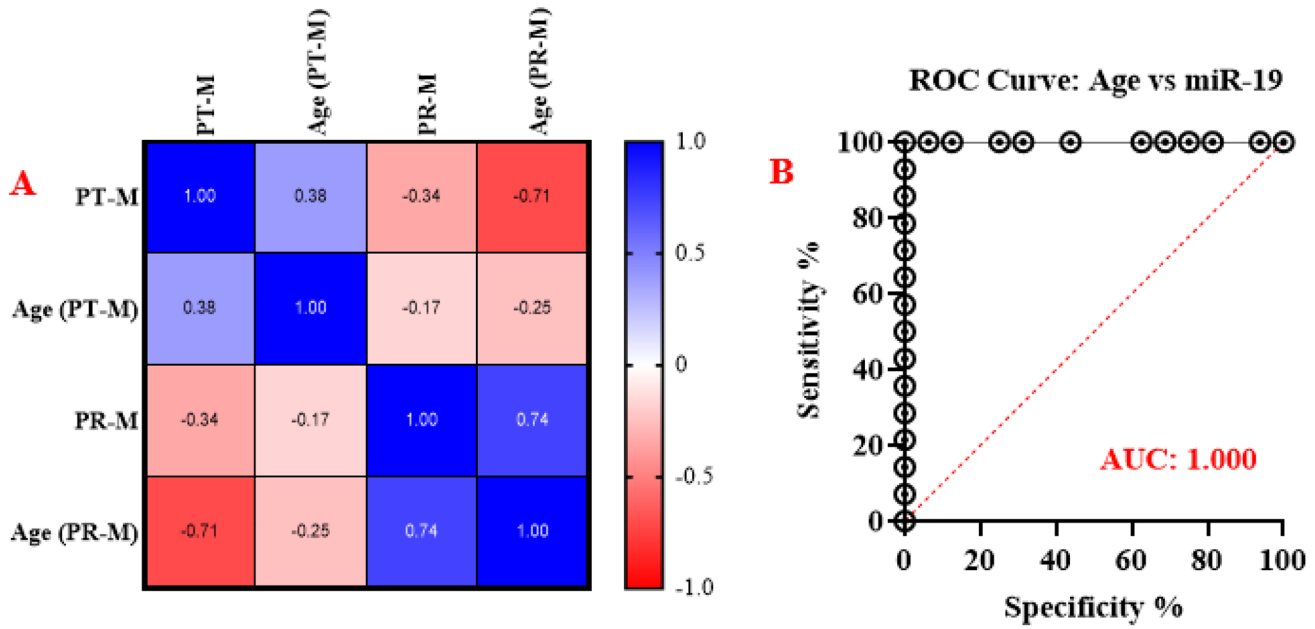


Fig. 8 The multiple matches squire plot (**A**) illustrates the Pearson correlation coefficient (*r*) between miR-19b and age in each of the four scenarios. (**B**) The receiver operating characteristics (ROC) curve for the miR-19b in combination with age vs. PR-M and PT-M women for every donor. With a 95% confidence interval (1.000 to 1.000) and an AUC of 1.000, there is a significant difference between PR-M and PT-M ($P < 0.0001$)

we found that there was a substantial difference in miR-19b expression between the PR-M and PT-M groups in response to estrogen levels. This shows that the expression of miR-19b varies between these two groups and is also strongly correlated with changes in estrogen levels, pointing to a possible function for miR-19b in regulating or reflecting changes linked to estrogen in these circumstances.

Lephart et al. [25] state that women's estrogen levels peak in their mid- to late-20s and subsequently drop by around 50% by the time they are 50 years old. When menopause occurs, this reduction intensifies and causes older women's estrogen levels to drop dramatically. This decrease in estrogen can have significant impacts on a range of physiological functions and medical disorders, emphasizing how crucial it is for women to comprehend and control their estrogen levels throughout their lives.

Conclusion

The study concludes by showing a substantial correlation between age and estrogen levels in female donors from the South Indian population and the expression levels of exosomal miR-19b. These results add to the body of data supporting the involvement of miR-19b in bone health and verify earlier research. In particular, the work shows that miR-19b downregulation may function as a highly useful biomarker for osteoporosis early diagnosis, providing opportunities for enhanced screening and intervention approaches in populations at risk.

Acknowledgements This study was supported by the Institutional Seed Research Grant at Nehru Memorial College (Project Code: NMC/Rand D Cell/2023-2024/06, March 2024). We express our gratitude to Government Medical College, Karur, India, for providing the necessary ethical clearance. We also thank the donors for supplying the samples for this study. Our sincere appreciation goes to the Core Facility Centre, Taipei Medical University, Taiwan, for providing the facilities for exosome characterization.

Funding Institutional Research Grant: NMC/Rand D Cell/2023–2024/06 March 2024.

Data availability Data will be made available upon reasonable request to the corresponding author.

Declarations

Conflict of Interest The authors declare no financial or non-financial competing interest.

Ethics Approval and Consent to Participate Approval document number: 2023/EC/R-0115, dated August 07, 2023.

References

1. Agrawal, T., & Verma, A. K. (2013). Cross sectional study of osteoporosis among women. *Medical Journal, Armed Forces India, 69*(2), 168–171. https://doi.org/10.1016/j.mjafi.2012.07.024

2. Khadilkar, A. V., & Mandlik, R. M. (2015). Epidemiology and treatment of osteoporosis in women: An Indian perspective. *International Journal of Women's Health, 7*, 841–850. https://doi.org/10.2147/IJWH.S54623
3. Bhadada, S. K., Chadha, M., Sriram, U., Pal, R., Paul, T. V., Khadgawat, R., et al. (2021). The Indian Society for Bone and Mineral Research (ISBMR) position statement for the diagnosis and treatment of osteoporosis in adults. *Archives of Osteoporosis, 16*(1), 102. https://doi.org/10.1007/s11657-021-00954-1
4. Kanis, J. A., WHO Study Group. (1994). Assessment of fracture risk and its application to screening for postmenopausal osteoporosis: Synopsis of a WHO report. *Osteoporosis International: A Journal Established as Result of Cooperation Between the European Foundation for Osteoporosis and the National Osteoporosis Foundation of the USA, 4*(6), 368–381. https://doi.org/10.1007/BF01622200
5. Schuit, S. C. E., van der Klift, M., Weel, A. E. A. M., de Laet, C. E. D. H., Burger, H., Seeman, E., et al. (2004). Fracture incidence and association with bone mineral density in elderly men and women: The Rotterdam Study. *Bone, 34*(1), 195–202. https://doi.org/10.1016/j.bone.2003.10.001
6. Kuo, T.-R., & Chen, C.-H. (2017). Bone biomarker for the clinical assessment of osteoporosis: Recent developments and future perspectives. *Biomarker Research, 5*, 18. https://doi.org/10.1186/s40364-017-0097-4
7. Hasanzad, M., Hassani, D. M., Rahbaran, M., Banihashemi, P., Fazeli, F., Ganji, M., et al. (2021). A systematic review of miRNAs as biomarkers in osteoporosis disease. *Journal of Diabetes and Metabolic Disorders, 20*(2), 1391–1406. https://doi.org/10.1007/s40200-021-00873-5
8. Iantomasi, T., Romagnoli, C., Palmini, G., Donati, S., Falsetti, I., Miglietta, F., et al. (2023). Oxidative stress and inflammation in osteoporosis: Molecular mechanisms involved and the relationship with microRNAs. *International Journal of Molecular Sciences, 24*(4), 3772. https://doi.org/10.3390/ijms24043772
9. Liu, D., Lin, Z., Huang, Y., & Qiu, M. (2022). Role of microRNA-19b-3p on osteoporosis after experimental spinal cord injury in rats. *Archives of Biochemistry and Biophysics, 719*, 109134. https://doi.org/10.1016/j.abb.2022.109134
10. Huda, M. N., Nafiujjaman, M., Deaguero, I. G., Okonkwo, J., Hill, M. L., Kim, T., et al. (2021). Potential use of exosomes as diagnostic biomarkers and in targeted drug delivery: Progress in clinical and preclinical applications. *ACS Biomaterials Science & Engineering, 7*(6), 2106–2149. https://doi.org/10.1021/acsbiomaterials.1c00217
11. Vadivalagan, C., Shitut, A., Kamalakannan, S., Chen, R.-M., Serrano-Aroca, Á., Mishra, V., et al. (2022). Exosomal mediated signal transduction through artificial microRNA (amiRNA): A potential target for inhibition of SARS-CoV-2. *Cellular Signalling, 95*, 110334. https://doi.org/10.1016/j.cellsig.2022.110334
12. Emmanuelle, N.-E., Marie-Cécile, V., Florence, T., Jean-François, A., Françoise, L., Coralie, F., et al. (2021). Critical role of estrogens on bone homeostasis in both male and female: From physiology to medical implications. *International Journal of Molecular Sciences, 22*(4), 1568. https://doi.org/10.3390/ijms22041568
13. Streicher, C., Heyny, A., Andrukhova, O., Haigl, B., Slavic, S., Schüler, C., et al. (2017). Estrogen regulates bone turnover by targeting RANKL expression in bone lining cells. *Scientific Reports, 7*(1), 6460. https://doi.org/10.1038/s41598-017-06614-0
14. Xiaoling, G., Shuaibin, L., & Kailu, L. (2020). MicroRNA-19b-3p promotes cell proliferation and osteogenic differentiation of BMSCs by interacting with lncRNA H19. *Bmc Medical Genetics, 21*(1), 11. https://doi.org/10.1186/s12881-020-0948-y
15. Yasamineh, S., Nikben, N., Hamed, A. M., Abdul, K. R., Kadhim, A.-A., & Hosseini, H. M. (2024). Increasing the sensitivity and accuracy of detecting exosomes as biomarkers for cancer monitoring using optical nanobiosensors. *Cancer Cell International, 24*(1), 189. https://doi.org/10.1186/s12935-024-03379-1
16. An, M., Wu, J., Zhu, J., & Lubman, D. M. (2018). Comparison of an optimized ultracentrifugation method versus size-exclusion chromatography for isolation of exosomes from human serum. *Journal of Proteome Research, 17*(10), 3599–3605. https://doi.org/10.1021/acs.jproteome.8b00479
17. Shi, H., Jiang, X., Xu, C., & Cheng, Q. (2022). Micrornas in serum exosomes as circulating biomarkers for postmenopausal osteoporosis. *Frontiers in Endocrinology, 13*, 819056. https://doi.org/10.3389/fendo.2022.819056
18. Yu, Y., Cai, W., Xu, Y., & Zuo, W. (2022). Down-regulation of miR-19b-3p enhances IGF-1 expression to induce osteoblast differentiation and improve osteoporosis. *Cellular and Molecular Biology (Noisy-Le-Grand, France), 68*(1), 160–168. https://doi.org/10.14715/cmb/2022.68.1.20
19. Liu, D., Wang, B., Qiu, M., & Huang, Y. (2021). MiR-19b-3p accelerates bone loss after spinal cord injury by suppressing osteogenesis via regulating PTEN/Akt/mTOR signalling. *Journal of Cellular and Molecular Medicine, 25*(2), 990–1000. https://doi.org/10.1111/jcmm.16159
20. Nilsson, S., Mäkelä, S., Treuter, E., Tujague, M., Thomsen, J., Andersson, G., et al. (2001). Mechanisms of estrogen action. *Physiological Reviews, 81*(4), 1535–1565. https://doi.org/10.1152/physrev.2001.81.4.1535
21. Rosenfeld, M. G., & Glass, C. K. (2001). Coregulator codes of transcriptional regulation by nuclear receptors. *The Journal of Biological Chemistry, 276*(40), 36865–36868. https://doi.org/10.1074/jbc.R100041200
22. Sun, M., Hu, L., Wang, S., Huang, T., Zhang, M., Yang, M., et al. (2020). Circulating microrna-19b identified from osteoporotic vertebral compression fracture patients increases bone formation. *Journal of Bone and Mineral Research, 35*(2), 306–316. https://doi.org/10.1002/jbmr.3892
23. Castellano, L., Giamas, G., Jacob, J., Coombes, R. C., Lucchesi, W., Thiruchelvam, P., et al. (2009). The estrogen receptor-alpha-induced microRNA signature regulates itself and its transcriptional response. *Proceedings of the National Academy of Sciences of the United States of America, 106*(37), 15732–15737. https://doi.org/10.1073/pnas.0906947106
24. Khosla, S., & Monroe, D. G. (2018). Regulation of bone metabolism by sex steroids. *Cold Spring Harbor Perspectives In Medicine, 8*(1), a031211. https://doi.org/10.1101/cshperspect.a031211
25. Lephart, E. D. (2018). A review of the role of estrogen in dermal aging and facial attractiveness in women. *Journal of Cosmetic Dermatology, 17*(3), 282–288. https://doi.org/10.1111/jocd.12508

Publisher's Note Springer Nature remains neutral with regard to jurisdictional claims in published maps and institutional affiliations.

Springer Nature or its licensor (e.g. a society or other partner) holds exclusive rights to this article under a publishing agreement with the author(s) or other rightsholder(s); author self-archiving of the accepted manuscript version of this article is solely governed by the terms of such publishing agreement and applicable law.